Journal of Alloys and Compounds 518 (2012) 86–95

Contents lists available at SciVerse ScienceDirect

Journal of Alloys and Compounds

journal homepage: www.elsevier.com/locate/jallcom

Effects of the constitution of CrON diffusion barrier on the oxidation resistance and interfacial fracture of duplex coating system

W.Z. Li [a,b,c,d,*], D.Q. Yi [a], Y.Q. Li [b], H.Q. Liu [a], C. Sun [c]

[a] School of Materials Science and Engineering, Central South University, Changsha 410083, China
[b] School of Materials Science and Engineering, Guangxi University, Nanning 530004, China
[c] State Key Laboratory for Corrosion and Protection, Institute of Metal Research, Chinese Academy of Sciences, Shenyang 110016, China
[d] SEG-CEMUC-Department of Mechanical Engineering, University of Coimbra, P-3030 788 Coimbra, Portugal

ARTICLE INFO

Article history:
Received 2 October 2011
Received in revised form
26 December 2011
Accepted 27 December 2011
Available online 3 January 2012

Keywords:
Duplex coatings
Diffusion barrier
Oxidation resistance
Interfacial strength
Interdiffusion

ABSTRACT

The duplex coating system of a NiCrAlY overlayer with a CrON diffusion barrier with different phase contents was deposited by AIP method. The duplex coatings were characterized regarding their microstructure, and the ability of the diffusion barrier was evaluated. The oxidation resistance and the interfacial strength of the duplex coatings were investigated. The results indicated that the duplex coating system with a diffusion barrier with an O/N ratio ~66 and a lower Cr_2O_3 phase content exhibited more excellent oxidation resistance and lesser interdiffusion than with a diffusion barrier with O/N ~30.1. The exposed coating samples possessed an improved interfacial strength compared with the annealed samples in the two duplex coating systems. The stronger interfacial strength in the coating system with a diffusion barrier with a low Cr_2O_3 phase content was related to the fewer defects and lower residual stress in the diffusion barrier.

1. Introduction

MCrAlY (M = Ni and/or Co) coatings, due to good balance between oxidation resistance and mechanical properties, have been widely used as standalone overlayers or bond coats in the TBCs for protecting the superalloy component in the gas turbine engine systems [1,2]. In order to further enhance the efficiency of the gas turbine engine system, the inlet temperature has been continuously increased. Consequently, the MCrAlY coatings degrade rapidly after a long-term exposure to elevated temperatures. The main cause is ascribed to strong interdiffusion between the coating and the substrate [3,4]. The introduction of a diffusion barrier as an interlayer in the interface between the MCrAlY coating and the substrate is considered as the most effective solution to limit the interdiffusion and thereby prolong the service lifetime of the coating.

The investigations on diffusion barriers over the past two decades indicated that for a diffusion barrier to be excellent it should combine the good barrier ability with the strong adhesion to the substrate or the overlayer [3–8]. Developing a diffusion barrier which can markedly suppress the interdiffusion and does not weaken largely the interfacial strength of the coating system onto the substrate is a key for the practical application of diffusion barrier, so that diffusion barriers, such as RuNiAl and NiCrAlON with the close compositions to the overlayers were fabricated [5,6].

In previous studies [4–8] it was found that the coating system of MCrAlY overlayer with a CrN diffusion barrier had a strong interfacial strength, but the oxidation resistance of the duplex coatings was limited. On the other hand, the introduction of a pure Cr_2O_3 diffusion barrier can suppress the interdiffusion with high efficiency due to the formation of a dense Al_2O_3 interlayer during thermal treatment, although the interfacial strength is impaired by the presence of residual stresses. Thus, one can expect that the CrON system with the appropriate phase ratio of CrN and Cr_2O_3 can provide an excellent diffusion barrier for the MCrAlY coating/Ni-based substrate system. Up to now, the effect of the CrON diffusion barrier with different phase contents on the oxidation resistance and the interfacial strength of the duplex coating system have not been investigated; thus an in-dept investigation on the mechanisms of oxidation and the interfacial properties of the MCrAlY overlayer with a diffusion barrier is desired.

In this work duplex coatings consisting of a MCrAlY coating and a CrON diffusion barrier, with different phase ratios of CrN and Cr_2O_3, were deposited on Ni-based superalloy by arc ion plating (AIP). In the present paper the microstructure of the MCrAlY coating and of the diffusion barrier was studied, and the oxidation resistance of the duplex coating and the effectiveness of the diffusion barrier were investigated. The interfacial strength of the coating systems

* Corresponding author. Tel.: +86 771 3270152; fax: +86 771 3270152.
E-mail address: wz-li@hotmail.com (W.Z. Li).

0925-8388/$ – see front matter © 2012 Elsevier B.V. All rights reserved.
doi:10.1016/j.jallcom.2011.12.139

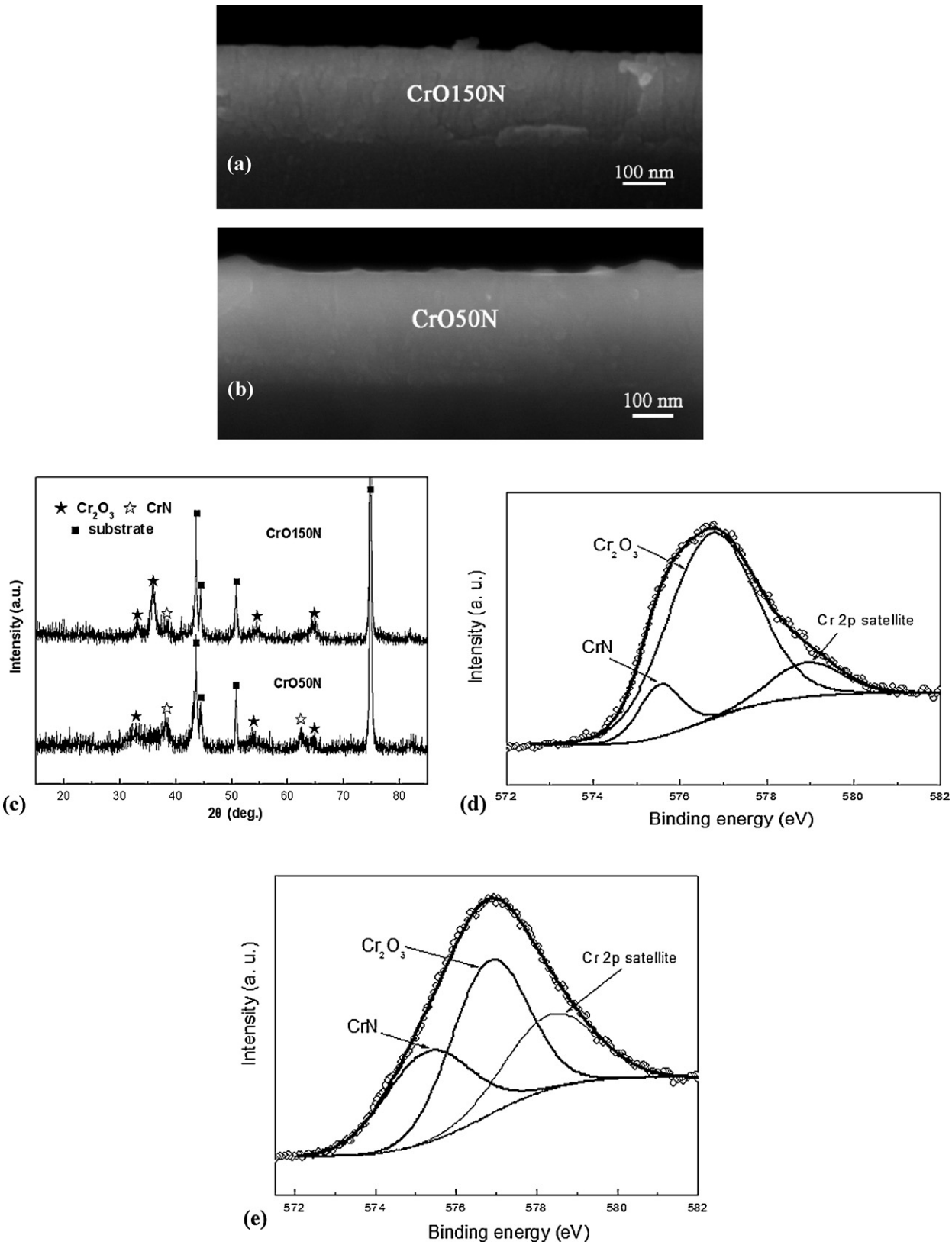

Fig. 1. Fractured cross-sectional SEM images ((a, b) on Si substrate), XRD patterns (c) and XPS patterns (d, e) of the as-deposited CrO150N (a, d) and CrO50N (b, e) diffusion barriers.

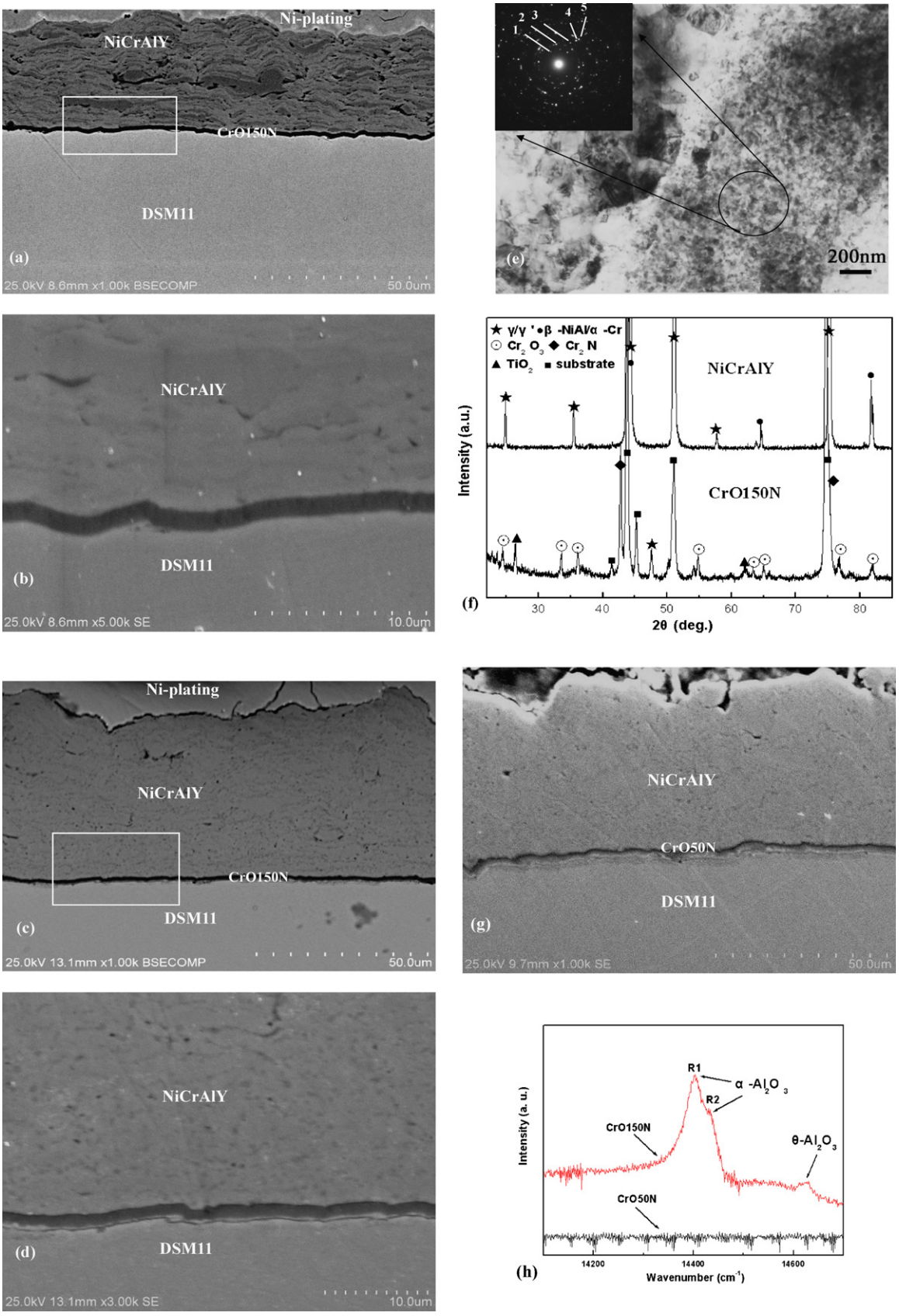

Fig. 2. Cross-sectional SEM images (a–d, g), TEM image (e), XRD patterns (f) and PSLS (h) of the as-deposited (a, b) and annealed (c–h) NiCrAlY/CrO150N/DSM11 (a–f) and NiCrAlY/CrO50N/DSM11 sample (g). (b, d) Show the magnified images of the selected zones in (a) and (c), respectively The inset SAD rings in (e) correspond to 1 (1 1 0), 2 (1 2 1), 3 (−1 1 0) plane of Cr_2O_3, and 4 (1 1 1), 5 (2 0 0) planes of γ/γ′.

Table 1
Composition (wt%) of the DSM11 substrate and the NiCrAlY alloy target.

Alloy	Ni	Cr	Co	Al	Ti	W	Mo	Ta	Y
DSM11	Bal	14	95	30	49	38	15	28	–
NiCrAlY	Bal	30	–	8	–	–	–	–	0.5

before and after thermal treatments was also evaluated and the interfacial fracture was discussed.

2. Experimental procedures

The Ni-based superalloy DSM11 was used as the substrate, whose composition is given in Table 1. Rectangular samples with dimensions of 15 mm × 10 mm × 2 mm (for oxidation test) and 50 mm × 8 mm × 15 mm (for bending test) were ground with 1000-grit SiC paper, grit-blasted in a wet atmosphere (200-mesh glass ball), then ultrasonically cleaned in ethanol and finally dried in air. The duplex coating system was deposited by arc ion plating (AIP) technique. Prior to deposition, the substrate was cleaned by Ar^+ ion bombardment for 5 min at a bias voltage of −800 V. The diffusion barriers were deposited from a pure Cr target in reactive atmosphere ($N_2 + O_2$). The total pressure that was used during deposition was 0.6 Pa. Two different O_2 flow rates were used, 150 mL/min and 50 mL/min, with balanced nitrogen being the diffusion barriers simply nominated as CrO150N or CrO50N, respectively. EDS results showed that the O/N ratio is higher in the CrO150N (O/N about 30.1) than in the CrO50N case (O/N around 66). The NiCrAlY overlayer was deposited using a NiCrAlY alloy target (the chemical composition is presented in Table 1) in an Ar^+ atmosphere at 0.3 Pa. The detailed deposition parameters for the diffusion barrier and the overlayer are shown in Table 2.

After deposition, the samples were heat-treated at 600 °C for 20 h and 900 °C for 4 h in a vacuum annealing furnace, and subsequently cooled down to room temperature. The heating rate was less than 7 °C/min. Intermittent isothermal oxidation tests were carried out at 1100 °C for 100 h in static air. After 10 h and 50 h, some samples were taken out for subsequent analysis. The weight gain was measured at various oxidation times. Accordingly, if oxide scales spalled from the surface during oxidation, the mass was counted together with that of the sample. The sensitivity of the balance used was 1×10^{-5} g.

The interfacial strength of the duplex coating was measured by three-point bending test on AG-I Universal Testing machine. The tests were performed in air at room temperature with a constant cross-head speed of 100 μm/min, and the samples were in a configuration which allowed the duplex coatings to be in tension [9]. The span of inner and outer dowel pins was 13 mm. An AE monitoring system was used to detect the damage events by mounting a sensitive resonant-type sensor on the lateral side of the sample. The gain was 50 dB and the threshold was selected as 50 dB. Before test, the sample was polished with 0.5 μm diamond paste to remove the coatings and oxides on the bottom surfaces and lateral sides. During test, since strong AE signals appeared, an in situ observation with an optical microscope was conducted in order to determine when to terminate the test. No less than three samples were tested for each load–displacement curve to ensure experimental accuracy.

The structures of the diffusion barrier and of the overlayer were analyzed by XRD. The morphologies and chemical compositions of the overlayer, diffusion barrier and oxide scales were observed and analyzed by using a scanning electron microscope (SEM) equipped with an energy-dispersive X-ray spectrum (EDS). The microstructure of the thermal annealed diffusion barriers was characterized by transmission electron microscopy (TEM). The chemical bonding of the elements present in the diffusion barrier was investigated by X-ray photoelectron spectroscopy (XPS), after the removal of the surface contamination layer by in situ Ar^+ sputtering during 200 s (and using 2 keV of energy). The identification of the Al_2O_3 phase in the diffusion barrier was done by studying the photo-stimulated luminescence spectra (PSLS) of the cross-section. The excitation source was a He–Ne laser with photon wavelength of 6328 nm. The incident laser beam was focused onto the sample surface with a laser spot of approximately 1 μm in diameter.

3. Results and discussion

3.1. Coatings characterization

3.1.1. Characterization of diffusion barriers

Fig. 1 shows the fractured cross-sectional SEM images, XRD and XPS spectra of the as-deposited CrO150N and CrO50N diffusion barriers. It is found that the CrO150N diffusion barrier presents a columnar structure (Fig. 1(a)), and the CrO50N diffusion barrier is compact and featureless (Fig. 1(b)). XRD patterns show that Cr_2O_3 and CrN phases are detected in the two diffusion barriers (Fig. 1(c)). From the intensity of diffraction peaks, it is observed that a higher content of Cr_2O_3 phase is present in the CrO150N diffusion barrier than that in the CrO50N. From the XPS spectra it is estimated that the Cr_2O_3/CrN ratio is 4 times higher in the CrO150N diffusion barrier than in the CrO50N (Fig. 1(d) and (e)). The presence of Cr2p satellite peaks in the XPS patterns is contributed to the low content of other chromium oxides [10].

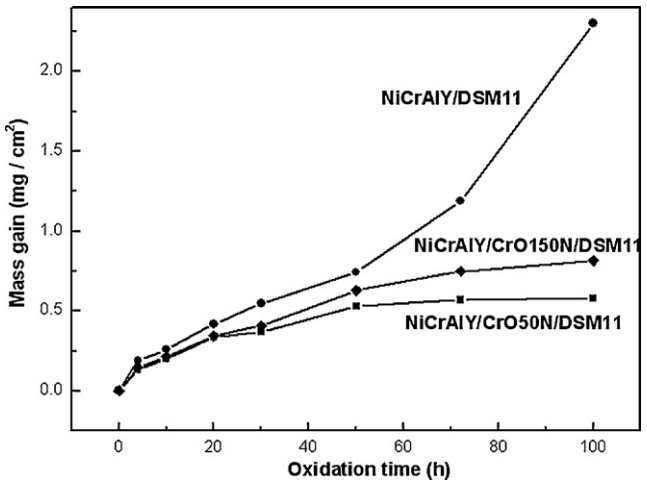

Fig. 3. Dependence of mass gain on time for the NiCrAlY/DSM11, NiCrAlY/CrO150N/DSM11 and NiCrAlY/CrO50N/DSM11 samples oxidized at 1100 °C for 100 h.

3.1.2. Microstructure of duplex coatings

The cross-sectional images presented in Fig. 2(a–d) shows that the CrO150N diffusion barrier is continuous and well adhered to the substrate and the overlayer. TEM observation reveals that the grains in the annealed diffusion barrier are about 50 nm and do not exhibit obvious preferred orientation (Fig. 2(e)). XRD analysis shows that Cr_2O_3 and Cr_2N are the two main phases in the annealed diffusion barrier, indicating that the CrN phase was transferred to Cr_2N during vacuum heat treatment [7]. After vacuum heat treatment, the NiCrAlY overlayer became compact (Fig. 2 (c)), and is mainly comprised of γ/γ′ and β-NiAl phases. Similarly, the CrO50N diffusion barrier in the NiCrAlY/CrO50N/DSM11 sample is continuous, dense with a good interfacial adhesion (Fig. 2(g)). The PSLS curves in Fig. 2(h) shows that no Al_2O_3 is formed in the annealed CrO50N diffusion barrier [11]. However, in the annealed CrO150N, low crystallinity α-Al_2O_3 and θ-Al_2O_3 is detected. It is known, the transformation of metastable θ-Al_2O_3 into stable α phase takes place at higher temperatures, and often induces the formation of growth stress in the diffusion barrier [7].

3.2. Isothermal oxidation kinetics

Fig. 3 shows the intermittent isothermal oxidation kinetics curves for the single NiCrAlY coating sample and the duplex coating samples with a CrO150N or CrO50N diffusion barrier. It is found that the three coating samples have a similar mass gain in the first 10 h. The strong increase in mass gain is attributed to the fast formation of alumina on the coating surface at the beginning of thermal exposure. From 10 h to 100 h, the single NiCrAlY coating has a pronounced mass gain. Slight scale spallation appeared at 70 h and apparent scale spallation was observed after 100 h exposure on the single coating surface. In comparison, no spallation was found on the two duplex coating samples during 100 h isothermal oxidation. The NiCrAlY coating with the CrO150N diffusion barrier exhibit a slight faster mass gain than that with the CrO50N diffusion barrier, especially after 30 h. The total mass gain for 100 h oxidation is 231 mg/cm^2, 0.82 mg/cm^2 and

Table 2
Deposition parameters of the duplex coatings.

	O_2 (mL/min)	Ar (mL/min)	Pressure (Pa)	Bias voltage (V)	Arc current (A)	Target	Time (min)
CrO150N	150	0	0.6	−240	65–75	Cr	40
CrO50N	50	0	0.6	−240	65–75	Cr	40
Overlayer	0	85	0.3	−240	65–75	NiCrAlY	360

0.58 mg/cm^2 for the NiCrAlY/DSM11, NiCrAlY/CrO150N/DSM11 and NiCrAlY/CrO50N/DSM11 sample, respectively. The isothermal oxidation kinetic curves clearly show that the introduction of a diffusion barrier can improve the oxidation resistance of the NiCrAlY coating. The duplex coating system with the CrO50N diffusion barrier exhibits a lower mass gain during 100 h oxidation.

3.3. Oxidation scales and element interdiffusion

Fig. 4 presents the surface SEM images and XRD patterns for the oxidation products on the duplex coating samples after isothermal oxidation for different time. From the surface images of 10 h oxidation (Fig. 4(a) and (b)), it is found that the morphology is rather similar for the two coating samples with the CrO150N and CrO50N diffusion barrier, which is due to the initial formation of surface oxides scales at the beginning of oxidation. After 50 h oxidation, cracks and spallation zones with a small area appear on the sample surface of the NiCrAlY/CrO150N coating (Fig. 4(c)). However, the surface oxides changed little on the sample with the CrO50N diffusion barrier (Fig. 4(d)). When the oxidation time was prolonged to 100 h, the scale spalling and crack propagation became aggravated on the NiCrAlY/CrO150N coating sample (Fig. 4(e)), however the oxide scales were kept in good condition for the sample with the CrO50N diffusion barrier (Fig. 4(f)). EDS detection revealed that the intact zones on the two samples have a very close chemical composition, such as A in Fig. 4(e) and B in Fig. 4(f), indicated in Table 3. However, in the spallation zone, for example C in Fig. 4(e), in addition to a higher content of Ni and Cr element, low contents of Co (0.67 at.%) and Ti (0.23 at.%) were detected, due to the diffusion from the substrate. The contents of other elements are listed in Table 3.

The XRD patterns in Fig. 4(g) and (h) shows that α-Al_2O_3 is the main oxidation product for the two duplex coating samples. On the 100 h exposed NiCrAlY/CrO150N coating sample, weak diffraction peaks of $NiCr_2O_4$ spinels were detected (Fig. 4(g)). Combined with the EDS analysis in Table 3, it is thought that $NiCr_2O_4$ spinels are formed in the spallation zone.

Fig. 5 presents the cross-sectional SEM images and element distribution for the duplex coating samples. It is clearly seen that Al_2O_3 scales are predominant at the outmost surface of the samples. The Al_2O_3 scales are about 3 μm in thickness and cracks are found in the scales of the NiCrAlY/CrO150N coating sample (Fig. 5(a)). A careful observation revealed that cracks are also present in the CrO150N diffusion barrier. The elemental line scanning results shows that there are low contents of alloy elements diffusing from the substrate in the NiCrAlY overlayer. Regarding Al and Ti elements, in addition to be rich in the diffusion barrier, they are in high contents in the interdiffusion zone (IZ) (Fig. 5(b)). Other studies confirmed that mixed oxides, mainly Al_2O_3 and TiO_2, are formed in the IZ [12]. Quantitative element analysis showed that the contents of Ti and Co in the NiCrAlY overlayer are 0.54 at.% and 231 at.%, respectively, and that the contents of Al, Ti and O in the CrO150N diffusion barrier are, 2865 at.%, 10.2 at.% and 539 at.%, respectively (more details in Table 4). Compared with the NiCrAlY/CrO150N coating sample, continuous, dense and thin (∼15 μm) Al_2O_3 scales well adhered to the coating surface are observed in the NiCrAlY/CrO50N case (Fig. 5(c)). The CrO50N diffusion barrier is sharp and no detectable defects are found. Only low contents of about 0.11 at.% Ti and 0.51 at.% Co were detected in the overlayer (see Table 4). The diffusion of Ti element from the substrate was suppressed by the diffusion barrier and high amounts of Ti are present in the IZ (5(d)). PSLS analysis in Fig. 6 confirmed the formation of corundum structure α-Al_2O_3 in the diffusion barrier of the two duplex coating samples. From the shift of R2 peak, it is estimated that a higher compressive residual stress is present in the CrO150N diffusion barrier, about −811 MPa more than that in the CrO50N diffusion barrier [11]. The presence of high residual stress led to the formation of cracks, which can be seen on Fig. 5(a), where apparent cracks are present in the CrO150N diffusion barrier. From the above results, it can be concluded that the NiCrAlY/CrO50N coating sample exhibited better oxidation resistance than the NiCrAlY/CrO150N coating sample. The CrO50N diffusion barrier showed stronger ability to suppress the interdiffusion than the CrO150N diffusion barrier.

Table 3
Chemical compositions (analyzed by EDS) of the different zones on the coating surface in Fig. 4(e) and (f) (at.%).

Element	Zone		
	A	B	C
O	5267	5100	4789
Al	3809	3948	30.14
Cr	392	364	775
Ni	500	564	1332

3.4. Oxidation resistance and diffusion barrier mechanism

The oxidation resistance of the MCrAlY coatings mainly depends on the formation of continuous, dense and adherent Al_2O_3 scales on the coating surface [1]. In particular, when the service temperature is elevated to 1100 °C, the integrity of surface Al_2O_3 scales is vital to commit the long-term protection of the coating. In the single coating system, the surface scales are apt to spall off in a rather short time due to the formation of TiO_2 comprising high growth stresses in the scales [5,13]. The repeated spalling and formation of surface Al_2O_3 scales will decrease the Al contents in the coating and, when the content of Al in the coating is too low, the continuous scales will not be regenerated. Thereby, mixed oxides of porous TiO_2 and $NiCr_2O_4$ spines can be formed, which allow the coating to be degraded gradually. Clearly, the Al reservoir in the coating is very important to ensure the integrity of surface scales. In the case of NiCrAlY overlayer with a CrON diffusion barrier, the Al level in the overlayer is mainly influenced by the diffusion: outward-diffusion to the coating surface to form and regenerate the surface Al_2O_3 scales and inward-diffusion into the diffusion barrier to replace Cr for the formation of Al_2O_3 diffusion barrier. When compared with the NiCrAlY/CrO50N sample, higher Al element from the overlayer was induced to migrate into the diffusion barrier to form Al_2O_3 in the coating sample with the CrO150N diffusion barrier, even at the stage of vacuum heat treatment. In fact, considering the samples with 100 h of exposition, higher Al contents (2865 at.%) were detected in the case of the CrO150N diffusion barrier, with only 463 at.% Al remaining in the NiCrAlY overlayer for this case, which indicated that more Al entered into the diffusion barrier and thus the Al level has decreased more rapidly in the NiCrAlY/CrO150N

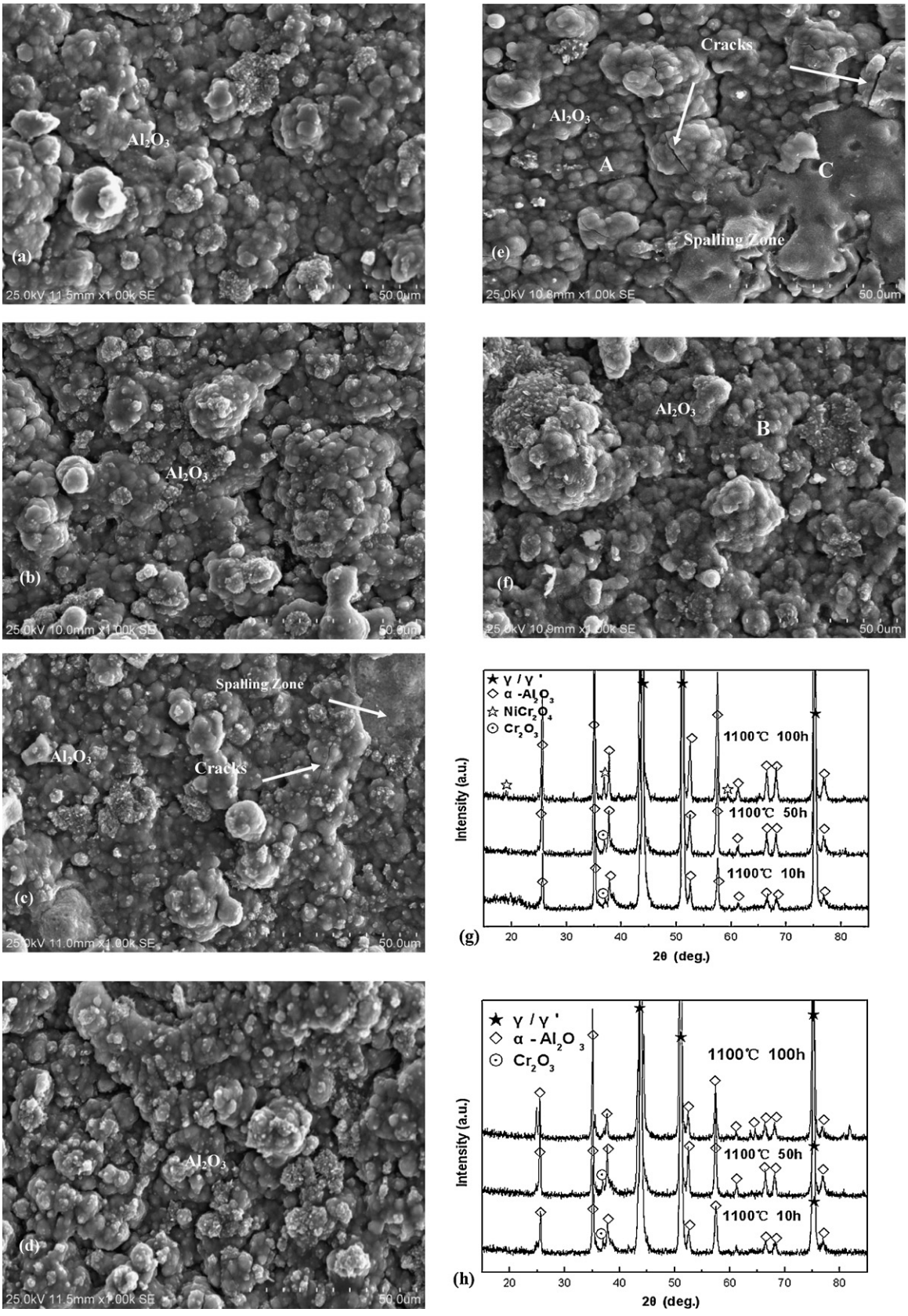

Fig. 4. Surface SEM images (a–f) and XRD patterns (g, h) of the duplex coating samples with the CrO150N (a, c, e, g) and CrO50N (b, d, f, h) diffusion barrier after isothermal oxidation for 10 h (a, b), 50 h (c, d) and 100 h (e, f) at 1100 °C.

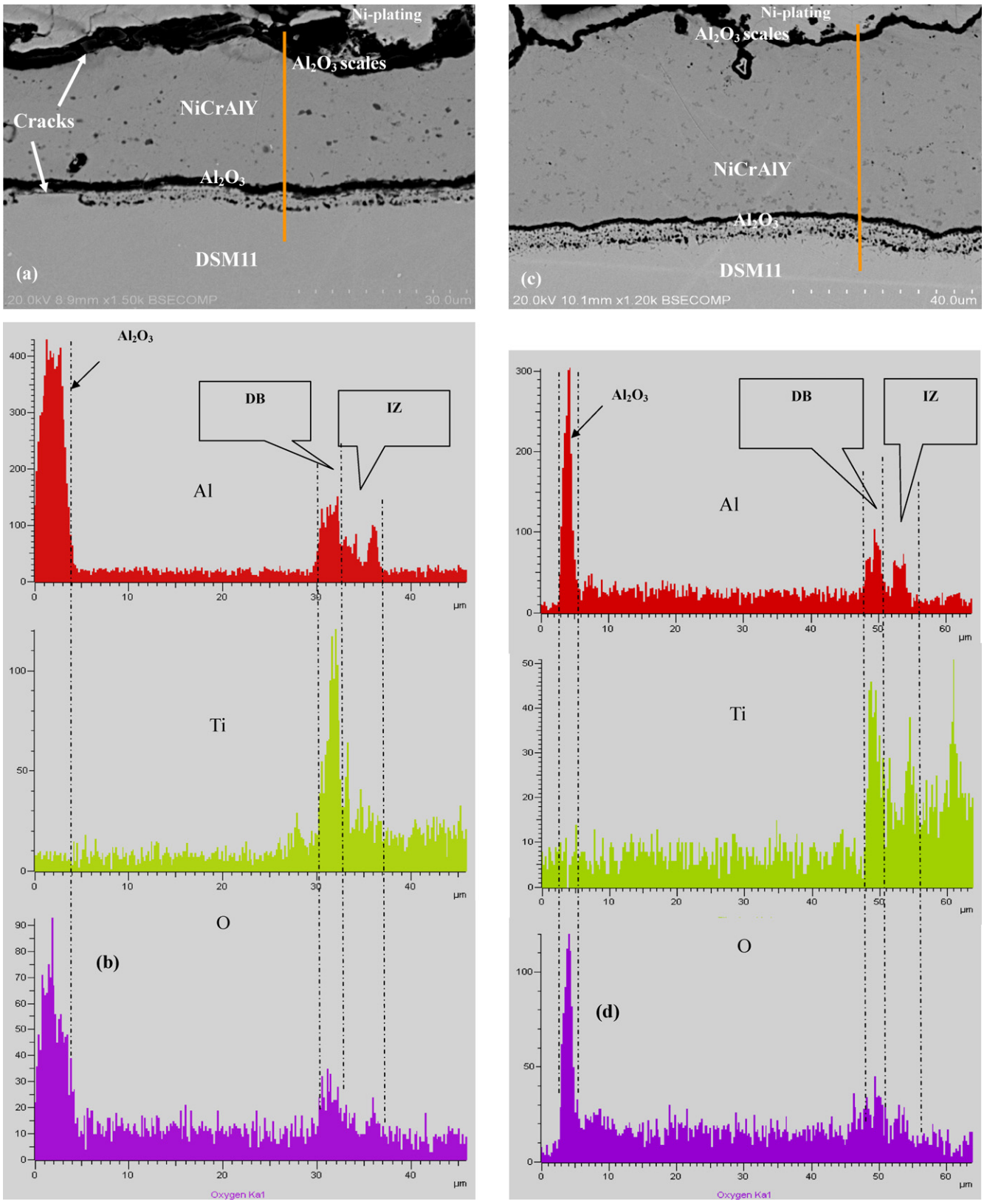

Fig. 5. Cross-sectional SEM images and corresponding EDS line scanning of the NiCrAlY/CrO150N/DSM11 (a, b) and NiCrAlY/CrO50N/DSM11 sample (c, d) after isothermal oxidation at 1100 °C for 100 h (diffusion barrier – DB; interdiffusion zone – IZ).

sample than the NiCrAlY/CrO50N sample. Moreover, affected by the combined effect of thermal stress from intermittent oxidation and growth stress from interdiffusion [5,7], the integrity of surface Al_2O_3 scales was undermined, and in this case the low level of Al element contributed to the ending of the self-healing process of the surface scales, thereafter the $NiCr_2O_4$ spines were formed in the NiCrAlY/CrO150N coating sample. Thus, the duplex coating system with the CrO150N diffusion barrier presented

Table 4
Average chemical compositions (analyzed by EDS) in the NiCrAlY coating and in the diffusion barriers after isothermal oxidation for 100 h (at.%).

Coatings		Al	Cr	Ti	Ni	Co	O
NiCrAlY/CrO50N	NiCrAlY	890	2837	0.11	60.03	0.51	208
	CrO50N	2181	990	667	1386	233	4543
NiCrAlY/CrO150N	NiCrAlY	463	2908	0.54	60.85	231	260
	CrO150N	2865	274	10.20	419	0.32	5390

weaker oxidation resistance than the NiCrAlY/CrO50N coating sample.

The ability of a diffusion barrier to suppress interdiffusion is related to the nature and microstructure of the materials selected. It is known that a dense, continuous and closed-packed structure Al_2O_3 exhibits outstanding diffusion barrier ability [4]. The presence of defects, such as grain boundaries, cracks and pores in the diffusion barrier will definitely decrease its competence due to the increase of short-circuit diffusion paths [14]. From the SEM images, it is clearly seen that a high density of defects is present in the columnar structure of the CrO150N diffusion barrier. Moreover, due to the formation of cracks in this barrier during thermal exposure, higher contents of alloy elements diffused from the substrate to the overlayer through the diffusion barrier. Thus, the CrO50N diffusion barrier exhibited stronger barrier ability than the CrO150N diffusion barrier.

3.5. Mechanical behavior during bending test

Fig. 7 illustrates the typical load–displacement curves for the annealed and 100 h exposed coating samples with CrON diffusion barriers. It is clear that the load increases linearly with the applied displacement in the annealed samples. Once a critical load is reached, a sharp drop of load occurs in the load–displacement curve. From the curves, it is found that the critical load is about 380 N and 455 N for the annealed duplex coating sample with the CrO150N and CrO50N diffusion barrier, respectively. However, an in situ observation combined with AE signal detection revealed that the sample with the CrO50N diffusion barrier has fractured along the diffusion barrier at the load of 410 N. The two annealed samples exhibited very similar mechanical behavior during bending test.

Interestingly, the 100 h exposed samples experienced characteristic three-stage deformation behavior during bending test: I – elastic deformation stage, the load increases linearly with the displacement; II – transition stage, the load decreases slowly with the increase of displacement; III – plastic deformation stage, the load almost keeps constant with the increase of displacement. From Fig. 7, it is clearly seen that both the samples with diffusion barrier presents a very close elastic deformation stage. At the stage II, the load decreases slightly faster with the displacement in the NiCrAlY/CrO150N coating sample than with the NiCrAlY/CrO50N coating sample. At the stage III, the two samples experienced a serious plastic deformation before damage. The displacement was 118 mm and 143 mm for the NiCrAlY/CrO150N and NiCrAlY/CrO50N coating sample, respectively, when the fracture occurred. Of course that the exposed samples have a far different deformation process from the annealed samples, and the sample with the CrO50N diffusion barrier experienced a more serious plastic deformation than that with the CrO50N diffusion barrier during bending test.

3.6. Interfacial damage and interfacial strength analysis

When a sudden drop of load or strong AE signals were detected during bending test, the coating sample was unloaded, and thereafter it was observed by SEM. Fig. 8 shows the cross-sectional SEM images of the duplex coating samples after unloading. It is clear that the fracture took place in the interface of the annealed coating sample (Fig. 8(a)). Moreover since no apparent damage was observed in the NiCrAlY overlayer [15].

Different from the annealed sample, the exposed sample underwent three-stage deformation during bending test. Before the drop of applied load, the sample has experienced a serious plastic deformation. SEM images showed that not only the interfacial fracture is present in the interfaces, but also that the propagation of perpendicular cracks into the overlayer occurs (Fig. 8(b) and (d)). By etching the samples with acids, the slip bands are found emerged

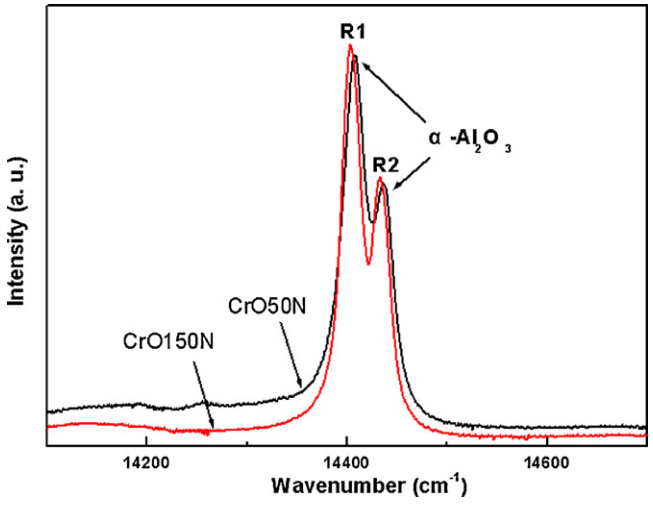

Fig. 6. PSLS for the diffusion barriers in the 100 h exposed samples.

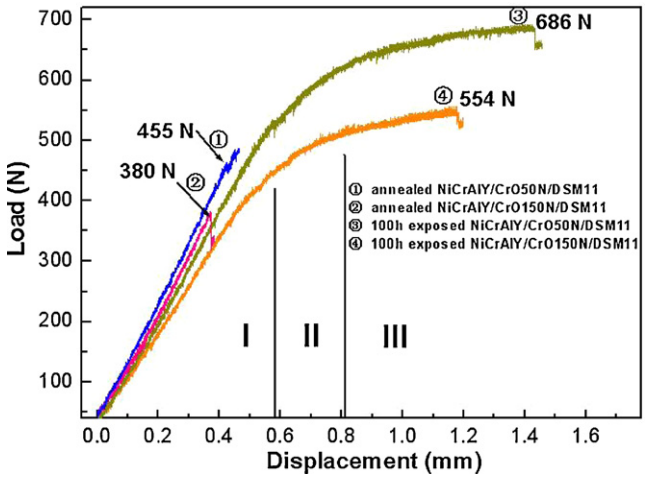

Fig. 7. Typical load–displacement curves for the annealed and 100 h exposed NiCrAlY/CrO150N/DSM11 and NiCrAlY/CrO50N/DSM11 samples during three-point bending test.

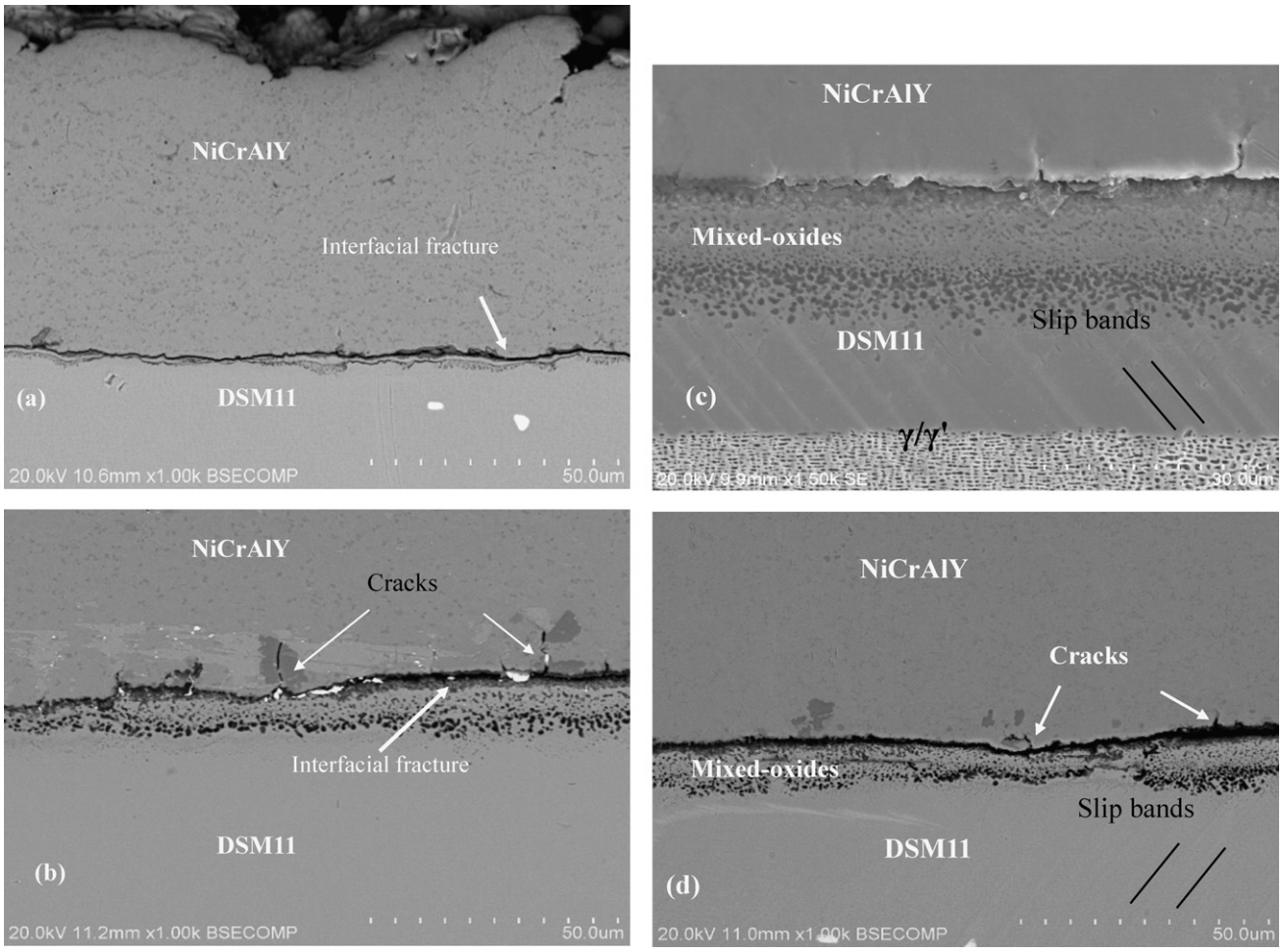

Fig. 8. SEM images of the NiCrAlY/CrO150N/DSM11 (a, b, c) and NiCrAlY/CrO50N/DSM11 (d) after three-point bending test; (a) as-annealed; (b, c, d) 100 h exposed, and (c) being etched for 15 s using the mixture of HNO_3 and HF.

on the substrate (Fig. 8(c)), which can be explained as the result of the serious plastic deformation during bending test. The results showed that the interfaces are still the weak part in the exposed duplex coating sample. However, higher plastic deformation was attained before the damage. The NiCrAlY/CrO50N coating sample exhibited a stronger resistance to fracture than the sample with the CrO150N diffusion barrier.

It is known that the interfacial strength is mainly influenced by the interfacial residual stress, which is principally originated from the different properties of layer materials [16]. In the present NiCrAlY/CrON/DSM11 system, the CrON layer is brittle ceramic material with a low CTE and high hardness, different from the ductile superalloy with a high CTE in the overlayer and the substrate. During the coating deposition and afterwards thermal exposure, residual stresses are introduced and concentrated in the interfaces of the diffusion barrier and the overlayer or the substrate. Thus, undoubtedly the interfaces are vulnerable areas during bending tests. The fact that a slightly weaker interfacial strength is present in the NiCrAlY/CrO150N coating system than in the NiCrAlY/CrO50N coating system should arise from: (i) a higher density of defects in the columnar structure of the CrO150N diffusion barrier, (ii) increased stresses from the detectable transformation of metastable θ to stable α-Al_2O_3, and (iii) lower effect of N-stability in the CrO150N diffusion barrier [3]. Although element interdiffusion can improve the interfacial adhesion to some extent due to the metallurgical bonding [8], the key for determining the interfacial strength should be related to the microstructures and the residual stress in the diffusion barrier.

4. Conclusions

The duplex coatings of the NiCrAlY overlayer with a CrO150N or CrO50N diffusion barrier were deposited by AIP technique. The oxidation resistance and the interfacial strength of the two duplex coating systems were compared. The following conclusions can be made:

The CrON diffusion barrier consists of Cr_2O_3 and CrN phases. The CrO150N diffusion barrier exhibited a columnar structure and possessed a higher Cr_2O_3/CrN ratio than the CrO50N diffusion barrier.

The NiCrAlY/CrO50N exhibited better oxidation resistance than that the coating sample with the CrO150N diffusion barrier, due to the slow depletion of Al element in the overlayer. The stronger barrier ability of the CrO50N diffusion barrier is attributed to the lower density of defects.

The exposed duplex coating samples had an improved interfacial strength, when compared with the annealed samples. The stronger interfacial strength in the NiCrAlY/CrO50N system should be related to the lesser incorporation of defects and lower residual stress observed in the CrO50N diffusion barrier. Combining the strong barrier ability and the good interfacial strength, the CrO50N diffusion barrier with a low Cr_2O_3 phase acts as an excellent diffusion barrier.

Acknowledgments

This work was supported by National Natural Science Foundation of China (Grant Nos. 51001032 and 50971047), the Portuguese Foundation for the Science and Technology (FCT, SFRH/BPD/76925/2011), the China Postdoctoral Science Foundation (Grant No. 20100480945), the Postdoctoral Science Foundation of Central South University and Guangxi Science Foundation (Grant No. 2010GXNSFD013006), which is gratefully acknowledged. Thanks Dr Nuno Figueiredo from University of Coimbra for checking and editing this paper.

References

[1] J.R. Nicholls, MRS Bull. 28 (2003) 659–670.
[2] N.P. Padture, M. Gell, E.H. Jordan, Science 296 (2002) 280–284.
[3] H. Peng, H.B. Guo, J. He, S.K. Gong, J. Alloys Compd. 502 (2010) 411–416.
[4] W.Z. Li, Y. Yao, Q.M. Wang, Z.B. Bao, J. Gong, C. Sun, X. Jiang, J. Mater. Res. 23 (2008) 341–352.
[5] W.Z. Li, Y.Q. Li, Q.M. Wang, C. Sun, X. Jiang, Corros. Sci. 52 (2010) 1753–1761.
[6] B. Bai, H.B. Guo, H. Peng, L.Q. Peng, S.K. Gong, Corros. Sci. 53 (2011) 2721–2727.
[7] W.Z. Li, Y.Q. Li, C. Sun, Z.L. Hu, T.Q. Liang, W.Q. Lai, J. Alloys Compd. 506 (2010) 77–84.
[8] W.Z. Li, Y. Yao, Y.Q. Li, J.B. Li, J. Gong, C. Sun, X. Jiang, Mater. Sci. Eng. A 512 (2009) 117–125.
[9] M.V.D. Burg, J. Th M.D. Hosson, Interface Sci. 3 (1995) 107–118.
[10] NIST data base, http://srdatanistgov/xps/.
[11] R.J. Christensen, D.M. Lipkin, D.R. Clarke, K. Murphy, Appl. Phys. Lett. 69 (1996) 3754–3756.
[12] W.Z. Li, Y.Q. Li, D.Q. Yi, H.Q. Liu, Adv. Mater. Res. 239–242 (2011) 206–213.
[13] P.S. Liu, K.M. Liang, S.R. Gu, Corros. Sci. 43 (2001) 1217–1226.
[14] R.W. Balluffi, S.M. Allen, W. Craig Carter, Kinetics of Materials, John Wiley & Sons, Inc., Hoboken, NJ, 2005.
[15] Z.H. Gan, S.G. Mhaisalkar, Z. Chen, S. Zhang, Z. Chen, K. Prasad, Surf. Coat. Technol. 198 (2005) 85–89.
[16] R.F. Bunshah, Handbook of Hard Coatings: Deposition Technologies, Properties and Applications, Noyes Publications/William Andrew Publishing, LLC Norwich, New York, 2001, p. 200.